

Simulation Study on the Effect of Multi-layer Biological Tissue on Focus Shift in High-Intensity Focused Ultrasound Therapy

Hu Dong^{1*}, Jiwen Hu², Gaofeng Peng¹, Qi Chen¹, Qiaolai Tan³

1. School of Information Science and Engineering, Changsha Normal University, Changsha 410100, China
2. School of Mathematics and Science, Nanhua University, Hengyang, 421001, China
3. School of Physics and Electrical Engineering, Xiangnan University, Chenzhou 423099, China

ARTICLE INFO

Article type:
Original Paper

Article history:

Received: Aug 27, 2022
Accepted: Feb 09, 2023

Keywords:

High-Intensity Focused
Ultrasound
Nonlinear
Acoustic Propagation
Focal Point

ABSTRACT

Introduction: During the treatment of soft tissue tumors with high-intensity focused ultrasound (HIFU), the focus may shift away from the desired point due to tissue heterogeneity. By studying the effect of biological tissue on focus shift, it can provide a theoretical basis for the safety and reliability of HIFU therapy.

Material and Methods: The finite difference time domain (FDTD) method was used to construct the simulation model of HIFU irradiated multi-layer biological tissue. Based on the Westervelt nonlinear acoustic propagation equation, the focus position change caused by the thickness of biological tissue and ultrasonic transducer during HIFU irradiation were simulated and calculated. The effects of ultrasonic transducer's electric power, irradiation frequency and tissue thickness on the focus position shift were analyzed and discussed.

Results: With the increase of electric power of HIFU transducer, the sound pressure at the focal point rose and the focal point approached the transducer side. With the increase of irradiation frequency of transducer, the sound pressure at the focus increased and the focus shifted away from transducer. With the increase of the thickness of biological tissue, the amplitude of sound pressure at the focal point decreased gradually. If the sound velocity of biological tissue was greater than that of water, the focus was close to the transducer side. If the sound velocity of biological tissue was less than the sound velocity of water, the focus moved to the side away from the transducer. For biological tissue with sound velocity greater than (or less than) water, the greater the sound velocity, the greater the relative shift distance difference of focal position.

Conclusion: As the electric power and frequency of ultrasonic transducer increased, the focus of HIFU moved toward and away from the transducer, respectively. For multi-layer biological tissue, the focus shift direction depended on the sound velocity relationship between biological tissue and water.

► Please cite this article as:

Dong H, Hu J, Peng G, Chen Q, Tan Q. Simulation Study on the Effect of Multi-layer Biological Tissue on Focus Shift in High-Intensity Focused Ultrasound Therapy. Iran J Med Phys 2023; 20: 341-350. 0.22038/IJMP.2023.67536.2173.

Introduction

High-intensity focused ultrasound (HIFU) can make the temperature of the diseased tissue rise above 70 °C in a short time, thus directly ablating the diseased tissue [1-3]. HIFU treatment technology has been applied to the clinical treatment of a variety of solid tumors, including superficial soft tissue tumors, prostate cancer, uterine leiomyoma, etc. as a non-invasive method, it has attracted much attention [4-6]. However, due to the differences in the electric power, irradiation frequency, thickness difference of biological tissue, the focus shift of the treatment area may occur in clinical treatment. For example, in the treatment of liver cancer nodules behind the ribs and adjacent large blood vessels, gallbladder, extrahepatic bile duct and gastrointestinal tract, if the location of HIFU treatment cannot be accurately predicted, it is likely to damage adjacent important tissue structures. In order to achieve accurate treatment, it is necessary to study the effects of the electric power, irradiation

frequency and thickness of biological tissue on the focal shift of HIFU.

Numerical simulation is an effective method to predict the distribution of acoustic field in HIFU treatment. Many scholars have studied the changes of focal field during HIFU treatment. Hynynen et al. found that at lower frequencies, the ultrasound beam can be effectively focused through the skull, but the position of the focus may be shifted by several millimeters from its predicted geometric position [7]. On the basis of considering the temperature-dependent dynamic sound velocity, Hallaj et al. found that there was thermoacoustic lens effect in the liver with fat layer by comparing the sound field of liver with and without fat layer, and the acoustic focus moved 2 mm to the transducer position [8]. Aubry et al. studied the adaptive ultrasonic focusing of sound waves through ribs under low-power HIFU irradiation through in vitro experiments. The pressure field in the focal plane was affected by nonuniform attenuation

*Corresponding Author: Tel: +86-0731-84036108; Email: wjd3203@163.com

and phase distortion. The average 2 mm shift of the main lobe was observed [9]. Okita et al. developed a HIFU simulator to simulate the transcranial HIFU treatment of brain tumors. It was found that the focus was shifted due to tissue heterogeneity and the focused ultrasound was diffused [10]. Narumi R et al. estimated the focal length error after propagation through breast issue and believed that the focal length error in breast tissue was caused by acoustic nonuniformity [11].

Based on the above research status, the finite difference time domain (FDTD) method is used to simulate the acoustic field, and the change of ultrasonic focusing position is studied when multi-layer biological tissue is in HIFU acoustic channel. To analyze the influence of the electric power, frequency, and thickness of the ultrasonic transducer on the focus position and accurately predict the HIFU treatment position. This paper has certain reference value for the formulation and implementation of HIFU treatment plan and the analysis of the real sound field, which will help to improve the treatment accuracy of HIFU in the treatment of human related diseases.

Materials and Methods

Westervelt nonlinear acoustic equation

The propagation of sound waves in media follows Huygens Fresnel principle [12]. Westervelt equation is a nonlinear acoustic model for the propagation of finite amplitude acoustic waves in thermoviscous media, which is derived from the fluid motion equation [13,14]. Westervelt equation can be expressed as:

$$\nabla^2 p - \frac{1}{c^2} \frac{\partial^2 p}{\partial t^2} + \frac{\delta}{c^4} \frac{\partial^3 p}{\partial t^3} + \frac{\beta}{\rho c^4} \frac{\partial^2 p^2}{\partial t^2} = 0 \tag{1}$$

P is the sound pressure, ρ and c are the density and sound velocity, δ is the diffusion coefficient of sound, $\delta = 2\alpha c_0^3 / \omega^2$, where ω is the acoustic angular frequency and α is the acoustic absorption coefficient. $\beta = 1 + B/2A$ is the nonlinear coefficient. The first two terms in equation (1) are the d'Alembert operator acting on the sound pressure, which is used to

$$\frac{\partial^2 p}{\partial x^2} = \frac{1}{12(\Delta x)^2} [-30p_{i,j,k}^n + 16(p_{i+1,j,k}^n + p_{i-1,j,k}^n) - p_{i+2,j,k}^n - p_{i-2,j,k}^n] \tag{4}$$

$$\frac{\partial^2 p}{\partial y^2} = \frac{1}{12(\Delta y)^2} [-30p_{i,j,k}^n + 16(p_{i,j+1,k}^n + p_{i,j-1,k}^n) - p_{i,j+2,k}^n - p_{i,j-2,k}^n] \tag{5}$$

$$\frac{\partial^2 p}{\partial z^2} = \frac{1}{12(\Delta z)^2} [-30p_{i,j,k}^n + 16(p_{i,j,k+1}^n + p_{i,j,k-1}^n) - p_{i,j,k+2}^n - p_{i,j,k-2}^n] \tag{6}$$

$$\frac{\partial^3 p}{\partial t^3} = \frac{1}{2(\Delta t)^3} (5p_{i,j,k}^n - 18p_{i,j,k}^{n-1} + 24p_{i,j,k}^{n-2} - 14p_{i,j,k}^{n-3} + 3p_{i,j,k}^{n-4}) \tag{7}$$

$$\begin{aligned} \frac{\partial^2 p^2}{\partial t^2} &= \chi \left(\frac{\partial p}{\partial t} \right)^2 + 2p \frac{\partial^2 p}{\partial t^2} \\ &= \frac{2}{(\Delta t)^2} [(p_{i,j,k}^n - p_{i,j,k}^{n-1})^2 + p_{i,j,k}^n (p_{i,j,k}^{n+1} - 2p_{i,j,k}^n + p_{i,j,k}^{n-1})] \end{aligned} \tag{8}$$

describe the linear lossless propagation under the sound velocity of small signal ultrasonic waves. The third term is the loss term, which describes the heat conduction and viscosity of the media, and the fourth item describes the nonlinear distortion of ultrasonic waves. FDTD difference [15] is performed for equation (1), where ∇^2 is Laplace operator, which can be written as follow:

$$\begin{aligned} \nabla^2 &= \nabla \cdot \nabla = (i \frac{\partial}{\partial x} + j \frac{\partial}{\partial y} + k \frac{\partial}{\partial z})(i \frac{\partial}{\partial x} + j \frac{\partial}{\partial y} + k \frac{\partial}{\partial z}) \\ &= \frac{\partial^2}{\partial x^2} + \frac{\partial^2}{\partial y^2} + \frac{\partial^2}{\partial z^2} \end{aligned} \tag{2}$$

Where i , j and k are unit direction vectors of x , y and z , respectively. From equation (2), it can be obtained that $\nabla^2 p$ in equation (1) is:

$$\nabla^2 p = \frac{\partial^2 p}{\partial x^2} + \frac{\partial^2 p}{\partial y^2} + \frac{\partial^2 p}{\partial z^2} \tag{3}$$

Figure 1 is the distribution diagram of spatial computing cells in rectangular coordinate system. On this basis, the calculation space of acoustic wave propagation is distributed and gridded.

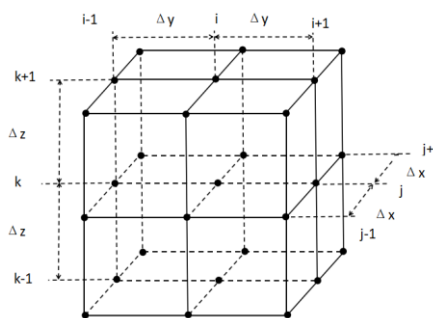


Figure 1. Spatial computation cell of FDTD in rectangular coordinate system

The differential terms in equations (1) and (3) are discretized by the finite difference time domain method as follow:

Where Δx , Δy and Δz respectively represent the spatial steps along the x -axis, y -axis and z -axis, Δt represents the time steps, i , j and k respectively represent the number of steps in the discrete space along the x , y and z -axis, and n represents the number of time steps. $P_{i,j,k}^n$ represents the instantaneous sound pressure at time $n\Delta t$ at coordinate $(i\Delta x, j\Delta y, k\Delta z)$. The explicit expression of the unknown term x can be obtained by substituting (4) - (6) into (1). The first-order Mur absorption boundary condition [16] is adopted for the boundary region:

$$\frac{\partial p}{\partial H} - \frac{1}{c} \frac{\partial p}{\partial t} = 0 \quad (9)$$

Where H may represent x , y , z directions, respectively. In the rectangular coordinate system, the calculation of three-dimensional sound field by Westervelt equation is very large, and the calculation time is also very long. For HIFU transducer, because of its axial symmetry, in order to simplify the calculation, the equation can be solved in two-dimensional r - z cylindrical coordinates to save the calculation time. In

cylindrical coordinates, $\nabla^2 p$ can be expressed as:

$$\nabla^2 p = \frac{\partial^2 p}{\partial r^2} + \frac{1}{r} \frac{\partial p}{\partial r} + \frac{\partial^2 p}{\partial z^2} \quad (10)$$

Where z represents the coordinate along the acoustic axis direction under the cylindrical coordinate, and r represents the coordinate perpendicular to the acoustic axis direction. Substitute equation (10) into equation (1) and use the finite difference time domain method to discretize the solution in cylindrical coordinates. The fourth-order accuracy is retained in space and the second-order accuracy is retained in time. The difference formula is as follow [15]:

$$\frac{\partial p}{\partial r} \approx \frac{1}{12\Delta r} (-p_{i,j+2}^n + 8p_{i,j+1}^n - 8p_{i,j-1}^n - p_{i,j-2}^n) \quad (11)$$

$$\frac{\partial^2 p}{\partial r^2} \approx \frac{1}{12(\Delta r)^2} (-p_{i,j+2}^n + 16p_{i,j+1}^n - 30p_{i,j}^n + 16p_{i,j-1}^n - p_{i,j-2}^n) \quad (12)$$

$$\frac{\partial^2 p}{\partial z^2} \approx \frac{1}{12(\Delta z)^2} (-p_{i+2,j}^n + 16p_{i+1,j}^n - 30p_{i,j}^n + 16p_{i-1,j}^n - p_{i-2,j}^n) \quad (13)$$

$$\frac{\partial p}{\partial t} \approx \frac{1}{2\Delta t} (3p_{i,j}^n - 4p_{i,j}^{n-1} + p_{i,j}^{n-2}) \quad (14)$$

$$\frac{\partial^2 p}{\partial t^2} \approx \frac{1}{(\Delta t)^2} (p_{i,j}^{n+1} - 2p_{i,j}^n + p_{i,j}^{n-1}) \quad (15)$$

$$\frac{\partial^3 p}{\partial t^3} \approx \frac{1}{(2\Delta t)^3} (6p_{i,j}^{n+1} - 23p_{i,j}^{n-1} + 34p_{i,j}^{n-2} - 24p_{i,j}^{n-3} + 8p_{i,j}^{n-4} - p_{i,j}^{n-5}) \quad (16)$$

The first-order Mur absorption boundary condition of formula (9) is adopted for the boundary. At the acoustic axis $r = 0$, symmetric boundary conditions are adopted for treatment:

$$\frac{\partial p}{\partial r} = 0 \quad (17)$$

By substituting (11) - (16) into equation (1), the explicit expression of unknown term $P_{i,j}^{n+1}$ can be obtained. Combined with boundary conditions (9) and (17), the two-dimensional sound field of HIFU transducer can be solved.

When the HIFU irradiation frequency is f , the corresponding acoustic absorption coefficient can be expressed as [17]:

$$\alpha(f) = \alpha_*(f/f_*)^\mu \quad (18)$$

In equation (17), α_* is the acoustic absorption coefficient corresponding to the media with acoustic frequency f_* . The index μ is usually 2 in water and 1.14 in biological tissue.

Establishment of simulation model

A two-dimensional axisymmetric geometric model of multi-layer biological tissue irradiated by HIFU transducer as shown in Figure 2 is established. The geometric focal length of HIFU ultrasonic transducer $F=11$ cm, the inner radius $r_1=2$ cm, and the outer radius $r_2=5$ cm. The irradiation frequency f (1 MHz~4 MHz) and the driving electric power P (100 W~700 w) of the ultrasonic transducer are adjustable. The multi-layer biological tissue is composed of water, skin, fat, connective tissue, muscle and liver, and their thickness are d_1 cm、 d_2 cm、 d_3 cm、 d_4 cm、 d_5 cm、 d_6 cm, respectively.

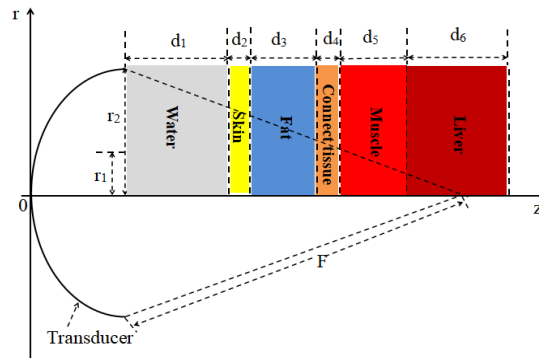


Figure 2. Simulation model of multi-layer biological tissue irradiated by HIFU

Table 1. Acoustic parameters of multi-layer media (1 MHz) [18-20]

Material properties	Units	Symbol	Water	Skin	Fat	connective tissue	Muscle	Liver
Density	kg/m ³	ρ	1000	1109	960	1525	1090	1036
Sound velocity	m/s	c	1482	1400	1476	1613	1547	1590
Absorption coefficient	dB/m	α	0.217	115	36	100	200	58
Nonlinear parameter	/	β	3.5	4.5	6.1	5.1	4.6	4.3

Simulation parameters

The sound field and focal position shift were simulated and calculated by MATLAB software (MathWorks, Natick, Massachusetts, United States). The acoustic parameters of relevant media were shown in Table 1.

Results

Figure 3, Figure 5, Figure 7, Figure 9, Figure 11, and Figure 13 showed the simulation results of sound pressure under different parameters such as electric power, frequency, and tissue thickness of ultrasonic transducer, respectively. The sound pressure had a direct impact on the focal temperature field. Figure 4, Figure 6, Figure 8, Figure 10, Figure 12, and Figure 14 showed the simulation calculation results of focus shift under different parameters such as electric power, frequency, and tissue thickness of ultrasonic transducer, respectively, and it was found that the changes of these parameters had a significant impact on the focus position shift of HIFU.

Influence of electric power change of ultrasonic transducer on focus shift

Under the condition of keeping the thickness of media unchanged, the influence of the electric power of ultrasonic transducer on the sound pressure and focus shift of HIFU was analyzed. Based on the model shown in Figure 2, the media thickness was $d_1=4$ cm, $d_2=1$ cm, $d_3=2$ cm, $d_4=1$ cm, $d_5=2$ cm, $d_6=1$ cm, respectively, and the irradiation frequency was $f = 1$ MHz. The simulation results were shown in Figure 3 and Figure 4. Figure 3 showed the axial sound pressure distribution. When the electric power was 100 W and 700 w, respectively, the sound pressure at the focal point increased from 6.96 MPa to 14.95 MPa, an increase of about 114.8%. Figure 4 showed the change of shift distance of the focus position relative to the focus position in the water area with electric power of ultrasonic

transducer, where "-" represented the movement of the focus toward the transducer. As can be seen from Figure 4, with the increase of the electric power of ultrasonic transducer, the focus position gradually moved toward the ultrasonic transducer.

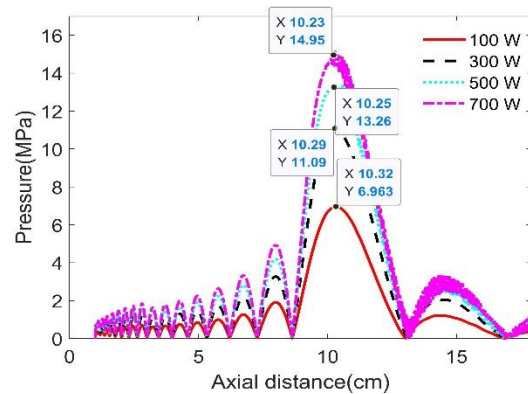


Figure 3. Comparison of axial sound pressure amplitude

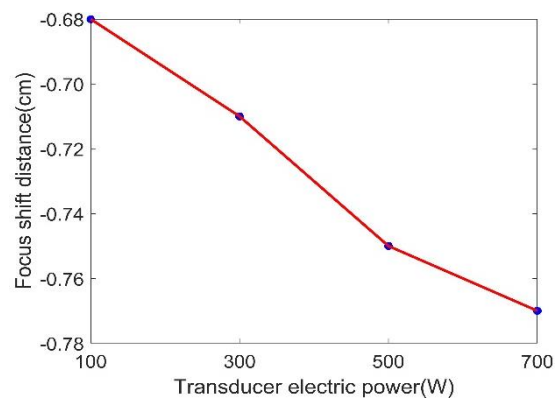


Figure 4. Shift of focus position with corresponding to electric power change

It can be seen from Figure 4 that when the electric power was 100 W and 700 W, respectively, the focal position in the non-linear case was shifted by 0.68 cm and 0.77 cm to the transducer direction relative to the focal position in water area, and their relative offset distance difference was 0.09 cm. As a result, it can be found that the change of electric power had little effect on the shift of focus position.

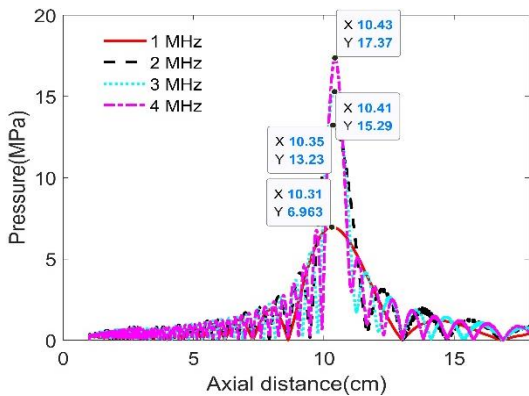


Figure 5. Comparison of axial sound pressure amplitude

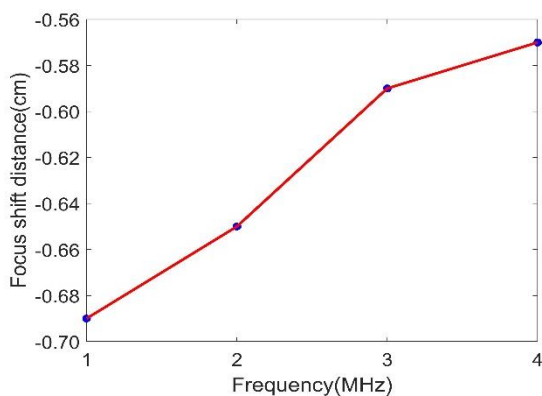


Figure 6. Shift of focus position with corresponding to irradiation frequency change

Effect of HIFU irradiation frequency change on focus shift

Under the condition of keeping the thickness of media unchanged, the influence of HIFU irradiation frequency on the sound pressure and focus shift of HIFU was analyzed. Based on the model shown in Figure 2, the media thickness was $d_1=4$ cm, $d_2=1$ cm, $d_3=2$ cm, $d_4=1$ cm, $d_5=2$ cm, $d_6=1$ cm, and the electric power was 100W. The simulation results were shown in Figure 5 and Figure 6. Figure 5 showed the axial sound pressure distribution. When the irradiation frequency was $f=1$ MHz and 4 MHz, respectively, the sound pressure at the focal point increased from 6.96 MPa to 17.40 MPa, an increase of about 150.0%. Figure 6 showed the shift distance of the focal position relative to the focal position in the water area as a function of frequency, where "-" represented the movement of the focal point toward the transducer. As can be seen from Figure 6, with the increase of irradiation frequency, the

focus position moved away from the ultrasonic transducer. It can be seen from Figure 6 that when the frequency was 1 MHz and 4 MHz, respectively, the focal position in the non-linear case was shifted by 0.69 cm and 0.57 cm away from the transducer in the direction of the focal position in water area, and the relative shift distance difference was 0.12 cm. Therefore, it can be found that the change of frequency had a great influence on the focal position shift.

Effect of biological tissue thickness change on focal shift (a) Skin

Keeping the electric power $P=100W$ and the irradiation frequency $f=1MHz$ constant and only changing the skin thickness, the influence on the sound pressure and the focus shift of HIFU was analyzed. Based on the model shown in Figure 2, the media thickness was $d_1=4$ cm, $d_3=2$ cm, $d_4=1$ cm, $d_5=2$ cm, and $d_6=1$ cm. The skin thickness was set to 1.0 cm, 1.1 cm, 1.2 cm, and 1.3 cm for simulation calculation, respectively, keeping the thickness of other tissue on the acoustic channel consistent. The simulation results were shown in Figure 7 and Figure 8.

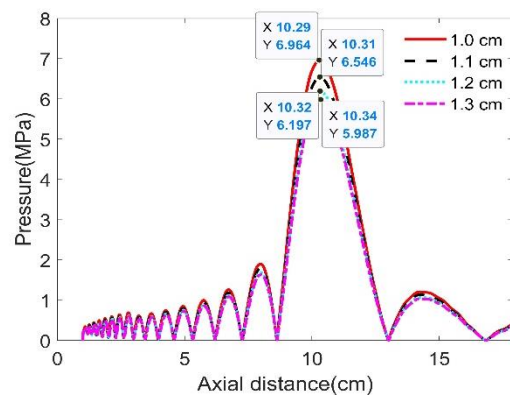


Figure 7. Comparison of axial sound pressure amplitude

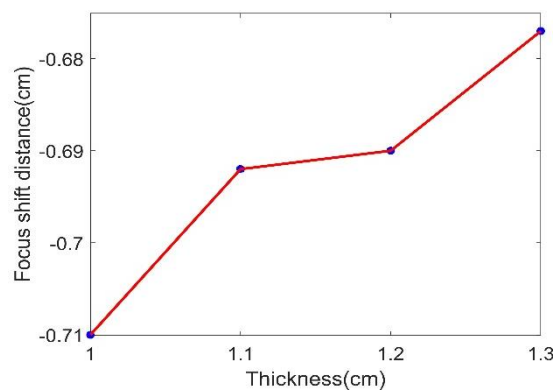


Figure 8. Shift of focus position with corresponding to skin thickness change

Figure 7 showed the axial sound pressure distribution. When the skin thickness was 1.0 cm and 1.3 cm, respectively, the sound pressure at the focal point decreased from 6.96 MPa to 5.99 MPa, a decrease of about 13.94%,

which was caused by tissue attenuation on the acoustic channel. Figure 8 showed the change of the shift distance of the focus position relative to the focus position in the water area with the thickness of the skin, where "-" represented the movement of the focus toward the transducer. As can be seen from Figure 8, as the thickness of the skin increased, the focus position moved away from the ultrasonic transducer. It can be seen from Figure 8 that when the fat thickness was 1.0 cm and 1.3 cm, respectively, the focal position in the non-linear case was shifted by 0.71 cm and 0.67 cm from the focal position in water area to the direction away from the transducer, and the relative shift distance difference was 0.04 cm. Thus, it can be found that the change of skin thickness had little influence on the shift of focus position.

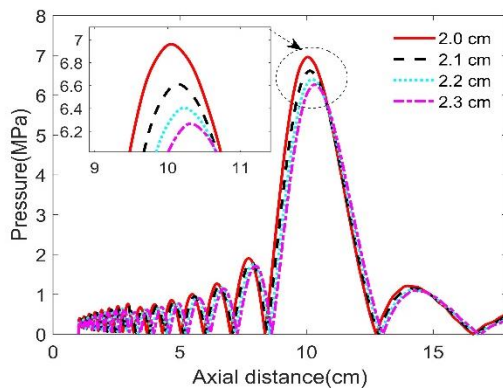


Figure 9. Comparison of axial sound pressure amplitude

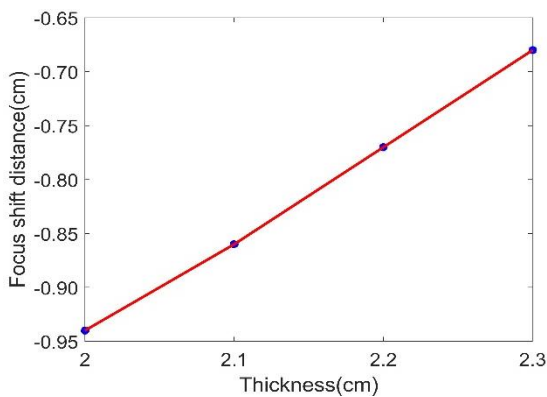


Figure 10. Shift of focus position with corresponding to fat thickness change fat thickness change

(b) Fat

Keeping the electric power $P = 100W$ and the irradiation frequency $f = 1MHz$ constant and only changing the fat thickness, the influence on the sound pressure and the focus shift of HIFU was analyzed. Based on the model shown in Figure 2, the media thickness was $d_1 = 4$ cm, $d_2 = 1$ cm, $d_4 = 1$ cm, $d_5 = 2$ cm, and $d_6 = 1$ cm. The fat thickness was set to 2.0 cm, 2.1 cm, 2.2 cm, and 2.3 cm for simulation calculation, keeping the thickness of other tissue on the acoustic channel consistent. The simulation results were shown in Figure 9 and Figure

10. Figure 9 showed the axial sound pressure distribution. When the fat thickness was 2.0 cm and 2.3 cm, respectively, the sound pressure at the focal point decreased from 6.96 MPa to 6.27 MPa, a decrease of about 9.91%, which was caused by tissue attenuation on the acoustic channel. Figure 10 showed the change of the shift distance of the focal position relative to the focal position in the water area with the thickness of the fat, where "-" represented the movement of the focal point toward the transducer. As can be seen from Figure 10, with the increase of fat thickness, the focus position moved away from the ultrasonic transducer. It can be seen from Figure 10 that when the fat thickness was 2.0 cm and 2.3 cm, respectively, the focal position in the non-linear case was shifted by 0.94 cm and 0.68 cm from the focal position in water area to the direction away from the transducer, and the relative shift distance difference was 0.26 cm. Therefore, it can be found that the change of fat thickness had a certain effect on the focal position shift.

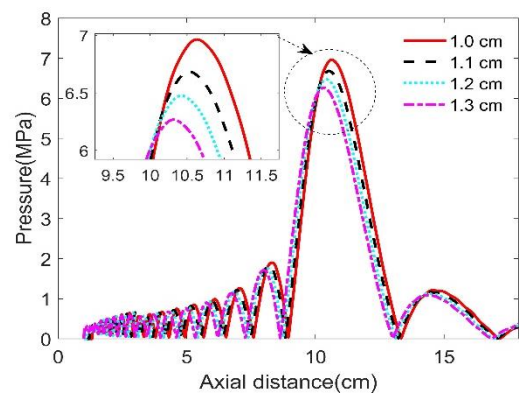


Figure 11. Comparison of axial sound pressure amplitude

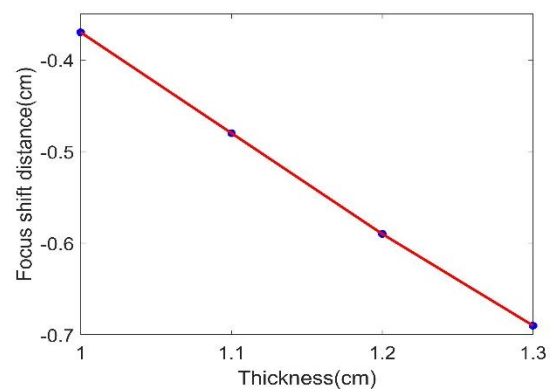


Figure 12. Shift of focus position with corresponding to connective tissue thickness change connective tissue

(c) Connective tissue

Keeping the electric power $P = 100W$ and the irradiation frequency $f = 1MHz$ constant and only changing the connective tissue thickness, the influence on the sound pressure and the focus shift of HIFU was analyzed. Based on the model shown in Figure 2, the media thickness was $d_1 = 4$ cm, $d_2 = 1$ cm, $d_3 = 2$ cm, $d_5 = 2$ cm,

and $d_6 = 1$ cm. The connective tissue thickness was set to 1.0 cm, 1.1 cm, 1.2 cm, and 1.3 cm for simulation calculation, respectively, keeping the thickness of other tissue on the acoustic channel consistent. The simulation results were shown in Figure 11 and Figure 12. Figure 11 showed the axial sound pressure distribution. When the thickness of the connective tissue was 1.0 cm and 1.3 cm, respectively, the sound pressure at the focal point decreased from 6.96 MPa to 6.28 MPa, a decrease of about 9.77%, which was caused by the attenuation of the tissue on the acoustic channel. Figure 12 showed the change of the shift distance of the focal position relative to the focal position in the water area with the thickness of the connective tissue, where "-" represented the movement of the focal point toward the transducer. As can be seen from Figure 12, with the increase of the thickness of the connective tissue, the focus position moved toward the ultrasonic transducer. It can be seen from Figure 12 that when the thickness of the connective tissue was 1.0 cm and 1.3 cm, respectively, the focal position in the non-linear case was shifted by 0.37 cm and 0.69 cm toward the transducer direction relative to the focal position in water area, and the relative offset distance difference was 0.32 cm. As a result, it can be found that the change of connective tissue thickness had a great impact on the focal position shift.

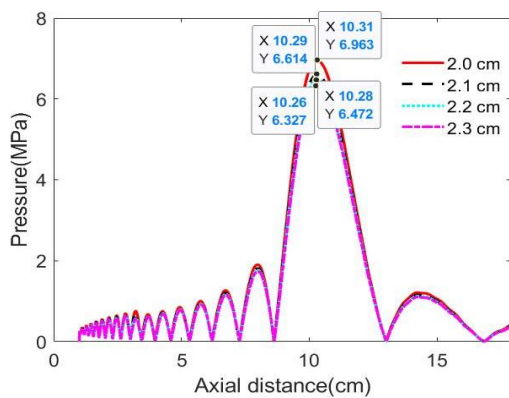


Figure 13. Comparison of axial sound pressure amplitude

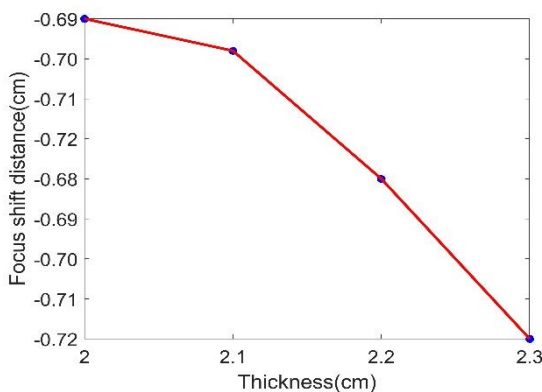


Figure 14. Shift of focus position with corresponding to muscle thickness change

(d) Muscle

Keeping the electric power $P = 100W$ and the irradiation frequency $f = 1MHz$ constant and only changing the muscle thickness, the influence on the sound pressure and the focus shift of HIFU was analyzed. Based on the model shown in Figure 2, the media thickness was $d_1 = 4$ cm, $d_2 = 1$ cm, $d_3 = 2$ cm, $d_4 = 1$ cm, and $d_6 = 1$ cm. The muscle thickness was set to 2.0 cm, 2.1 cm, 2.2 cm, and 2.3 cm for simulation calculation, respectively, keeping the thickness of other tissue on the acoustic channel consistent. The simulation results were shown in Figure 13 and Figure 14. Figure 13 showed the axial sound pressure distribution. When the muscle strength was 2.0 cm and 2.3 cm, respectively, the sound pressure at the focus decreased from 6.96 MPa to 6.34 MPa, a decrease of about 8.91%, which was caused by tissue attenuation on the acoustic channel. Figure 14 showed the change of the shift distance of the focus position relative to the focus position in the water area with the thickness of the muscle, where "-" represented the movement of the focus toward the transducer. As can be seen from Figure 14, with the increase of muscle thickness, the focus position moved toward the ultrasonic transducer.

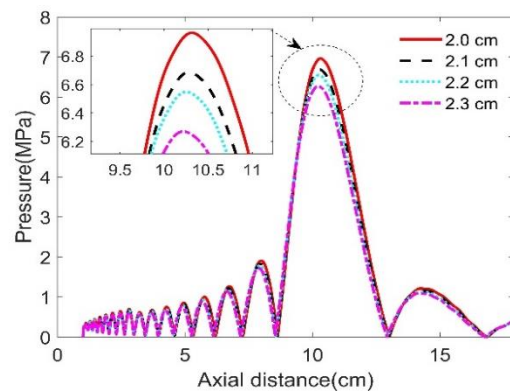


Figure 15. Comparison of axial sound pressure amplitude

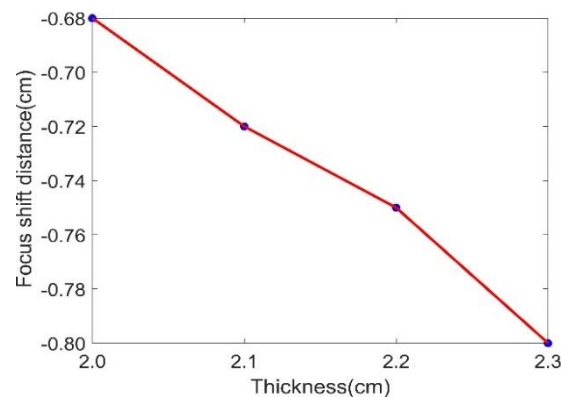


Figure 16. Shift of focus position with corresponding to liver thickness change

It can be seen from Figure 14 that when the muscle thickness was 2.0 cm and 2.3 cm, respectively, the focal position in the non-linear case was shifted by 0.69 cm and 0.72 cm to the transducer direction relative to the focal

position in water area, and the relative shift distance difference was 0.03 cm. Thus, so it can be found that the change of muscle thickness had little influence on the focal position shift.

(e) Liver

Keeping the electric power $P = 100\text{W}$ and the irradiation frequency $f = 1\text{MHz}$ constant and only changing the liver thickness, the influence on the sound pressure and the focus shift of HIFU was analyzed. Based on the model shown in Figure 2, the media thickness was $d_1 = 4\text{ cm}$, $d_2 = 1\text{ cm}$, $d_3 = 2\text{ cm}$, $d_4 = 1\text{ cm}$, and $d_5 = 2\text{ cm}$, respectively. The liver thickness was set to 2.0 cm, 2.1 cm, 2.2 cm, and 2.3 cm for simulation calculation, respectively, keeping the thickness of other tissue on the acoustic channel consistent. The simulation results were shown in Figure 15 and Figure 16. Figure 15 showed the axial sound pressure distribution. When the liver thickness was 2.0 cm and 2.3 cm, respectively, the sound pressure at the focal point decreased from 6.96 MPa to 6.26 MPa, a decrease of about 10.06%, which was caused by tissue attenuation on the acoustic channel. Figure 16 showed the change of the shift distance of the focal position relative to the focal position in the water area with the thickness of the liver, where "-" represented the movement of the focal point toward the transducer. As can be seen from Figure 16, with the increase of muscle thickness, the focus position moved toward the ultrasonic transducer. It can be seen from Figure 16 that when the liver thickness was 2.0 cm and 2.3 cm, respectively, the focal position in the non-linear case was shifted by 0.68 cm and 0.80 cm to the transducer direction relative to the focal position in the water area, and the relative shift distance difference was 0.12 cm. It can be seen that the influence of the liver thickness on the focal position was larger than that of the muscle thickness on the focal position shift.

Discussion

Usually, the beam generating array element or the acoustic lens would focus the ultrasonic beam energy [21, 22]. The ultrasonic wave must travel through multi-layer media, including skin, fat, connective tissue, muscle, and liver, before it can reach the diseased tissue area from the ultrasonic transducer. Owing to the vast variations in the acoustic properties of various media, there will be some degree of focus shifting as sound waves travel through them due to attenuation, reflection, and refraction [23]. The emphasis can be somewhat shifted further by the refraction of sound waves along the acoustic channel. This will exacerbate the patient's additional agony and result in needless complications for the real therapeutic procedure.

For biological tissue, there were a certain number of bubbles inside [26-28]. The higher the HIFU irradiation frequency, the weaker the bubble oscillation in biological tissue. The attenuation of bubble oscillation led to the reduction of ultrasonic attenuation and the shift of focus position [29]. In addition, the larger the

initial void fraction of the bubbles in the biological tissue, the larger the bubble number density, and the weaker the penetration of ultrasound through the bubble region. On the other hand, from the relationship between the acoustic absorption coefficient and the irradiation frequency (see equation (18)), the larger the irradiation frequency, the larger the acoustic coefficient. All these factors would lead to the increase of ultrasonic attenuation, and then led to the shift of HIFU focus position away from the transducer. This result was consistent with the research results in literature [30].

According to Snell's theorem, when the acoustic wave passed through another biological tissue from one layer, the acoustic wave would be refracted, so the addition of biological tissue would cause the focus to shift [24]. When the sound wave passed through the connective tissue from the fat, the refraction angle was large and inward, so the focus position would shift toward one end of the transducer. With the continuous increase of the thickness of the connective tissue, the longer the inward refraction path, the focus would further move toward one end of the transducer. It can be seen from Table 1 that, taking the sound velocity of water as a reference, the change of sound velocity of fat relative to the sound velocity of connective tissue was small, and the sound velocity of fat was smaller than that of water, while the sound velocity of connective tissue was larger than that of water. The refraction angle of the acoustic wave in the fat was small relative to the connective tissue, and the refraction direction was outward, which caused the focal position to move away from the transducer, and the change caused by the offset distance relative to the thickness of the connective tissue was small. Similarly, since the sound velocity of the skin was less than that of water, the external refraction angle of the sound wave in the skin was smaller than that of water, and with the continuous increase of the thickness of the skin, the focus position moved away from the transducer. While the sound velocity of muscle and liver was greater than that of water, the internal refraction angle of sound wave in muscle and liver was larger than that of water, and with the continuous increase of the thickness of muscle and liver, the focus position moved toward the transducer.

For single biological tissue (such as connective tissue, liver, and muscle) with a sound velocity greater than water in the acoustic channel, the greater the sound velocity, the greater the relative shift distance difference of the focus. The relative shift distance difference of connective tissue, liver and muscle was about 0.32 cm, 0.12 cm, and 0.03 cm, respectively. For single biological tissue (such as fat and skin) with sound velocity less than that of water in the acoustic channel, the greater the sound velocity, the greater the relative shift distance difference of focus, and the relative shift distance difference of fat and skin was about 0.26 cm and 0.04 cm, respectively. At the same time, the greater the acoustic absorption coefficient of biological tissue, the stronger the focus energy attenuation. With the increase of the thickness of biological tissue, the more significant

the shift of the focus in the direction of the acoustic axis, the greater the thickness, the greater the energy attenuation, that was, the greater the decrease of the acoustic pressure amplitude.

Conclusion

In this paper, the focal position of the acoustic beam after passing through multi-layer biological tissue during HIFU treatment was studied by simulation. The electric power, frequency and thickness of biological tissue irradiated by HIFU would cause the shift of focus position and the change of sound pressure amplitude, and their effects on the focal position of HIFU were analyzed and discussed. With the increase of electric power of HIFU transducer, the sound pressure at the focal point rose and the focal point approached the transducer side. With the increase of frequency of the transducer, the sound pressure at the focus increased and the focus shifted away from the transducer. As the tissue thickness increased and the biological tissue was the same tissue, and the sound velocity of tissue was greater than that of water, the focus moved to the HIFU transducer side, on the contrary, the focus moved to the side away from the HIFU transducer. The greater the thickness of biological tissue in the acoustic channel, the greater the acoustic attenuation at the focal point, and the more obvious the decrease of acoustic pressure amplitude. For biological tissue with sound velocity greater than (or less than) water, with the increase of its thickness, the greater the sound velocity, the greater the relative shift distance difference of the focus. This study will allow physicians to obtain the axial focus shift of the incident ultrasound prior to the procedure, which will help them determine whether the current HIFU transducer focus is in the lesion area, and further develop safer HIFU treatment protocols to improve treatment efficiency. Future research work will focus on experimental work, and we will create experimental conditions and conduct experimental studies to support the simulation results in this paper.

Acknowledgment

The Changsha Natural Science Foundation Project (grant No. kq2202313) and the Hunan Provincial Department of Education of China's Key Project (grant No. 21A0618) provided funding for this work. The anonymous reviewers' insightful remarks and recommendations are much appreciated by the authors.

References

1. Wang H, Zeng D, Chen Z, Yang Z. A rapid and non-invasive method for measuring the peak positive pressure of HIFU fields by a laser beam. *Scientific Reports*. 2017; 7(1):850. DOI: 10.1038/s41598-017-00892-4.
2. Zhao J, Shen H, Hu X, Wang Y, Yuan Y. The efficacy of a new high-intensity focused ultrasound therapy for metastatic pancreatic cancer. *International Journal of Hyperthermia*. 2021 Jan 1;38(1):288-95. DOI: 10.1080/02656736.2021.1876252.
3. Haddadi S, Ahmadian MT. Analysis of nonlinear acoustic wave propagation in HIFU treatment using Westervelt equation. *Scientia Iranica*. 2018 Aug 1;25(4):2087-97. DOI:10.24200/sci.2017.4496.
4. Marinova M, Feradova H, Gonzalez-Carmona MA, Conrad R, Tonguc T, Thudium M, et al. Improving quality of life in pancreatic cancer patients following high-intensity focused ultrasound (HIFU) in two European centers. *European Radiology*. 2021 Aug;31(8): 5818-29. DOI:10.1007/s00330-020-07682-z.
5. Xiao-Ying Z, Hua D, Jin-Juan W, Ying-Shu G, Jiu-Mei C, Hong Y, et al. Clinical analysis of high-intensity focussed ultrasound ablation for abdominal wall endometriosis: a 4-year experience at a specialty gynecological institution. *International Journal of Hyperthermia*. 2019 Jan 1;36(1):87-94. DOI:10.1080/02656736.2018.1534276.
6. Apfelbeck M, Clevert DA, Rieke J, Stief C, Schlenker B. Contrast enhanced ultrasound (CEUS) with MRI image fusion for monitoring focal therapy of prostate cancer with high intensity focused ultrasound (HIFU). *Clinical Hemorheology and Microcirculation*. 2018 Jan 1;69(1-2):93-100. DOI:10.3233/CH-189123.
7. Hynynen K, Jolesz F.A. Demonstration of Potential Noninvasive Ultrasound Brain Therapy Through an Intact Skull. *Ultrasound in Medicine & Biology*. 1998;24(2):275 – 83. DOI : 10.1016/S0301-5629(97)00269-X.
8. Hallaj I M, Cleveland R O, Hynynen K. Simulations of the thermo-acoustic lens effect during focused ultrasound surgery. *The Journal of the Acoustical Society of America*. 2001; 109(5):2245-53. DOI:10.1121/1.1360239.
9. Aubry JF, Pernot M, Marquet F, Tanter M, Fink M. Transcostal high-intensity-focused ultrasound: ex vivo adaptive focusing feasibility study. *Physics in Medicine & Biology*. 2008 May 12;53(11):2937. DOI:10.1088/0031-9155/53/11/012.
10. Okita K, Ono K, Takagi S, Matsumoto Y. Development of high intensity focused ultrasound simulator for large-scale computing. *International journal for numerical methods in fluids*. 2011 Jan 10;65(1-3):43-66. DOI:10.1002/fld.2470.
11. Narumi R, Matsuki K, Azuma T, Sasaki A, Takagi S, Matsumoto Y, et al. Numerical Estimation of HIFU Focal Error for Breast Cancer Treatment. 2013 IEEE International Ultrasonics Symposium (IUS). IEEE, 2013:926-9. DOI: 10.1109/ULTSYM.2013.0238.
12. Gluza M, Moosavi P, Sotiriadis S. Breaking of Huygens-Fresnel principle in inhomogeneous Tomonaga-Luttinger liquids. *Journal of Physics A: Mathematical and Theoretical*. 2022; 55(5): 054002. DOI:10.1088/1751-8121/ac39cc.
13. Solovchuk M, Sheu TWH, Thiriet M. Simulation of nonlinear Westervelt equation for the investigation of acoustic streaming and nonlinear propagation effects. *The Journal of the Acoustical Society of America*. 2013;134(5):3931-42. DOI:10.1121/1.4821201.
14. Norton GV, Purrington RD. The Westervelt equation with viscous attenuation versus a causal propagation operator: A numerical comparison. *Journal of sound and vibration*. 2009;327(1-2): 163-72. DOI:10.1016/j.jsv.2009.05.031.

15. Hallaj IM, Cleveland RO. FDTD simulation of finite-amplitude pressure and temperature fields for biomedical ultrasound. *Journal of the Acoustical Society of America*. 1999; 105(5):7-12. DOI:10.1121/1.426776.
16. Mur G. Absorbing Boundary Conditions for the Finite-Difference Approximation of the Time-Domain Electromagnetic-Field Equations. *IEEE Transactions on Electromagnetic Compatibility*. 2007; 23(4):377-382. DOI:10.1109/TEMC.1981.303970.
17. Namakshenas P, Afsaneh M. Microstructure-based non-Fourier heat transfer modeling of HIFU treatment for thyroid cancer. *Computer Methods and Programs in Biomedicine*. 2020; 197: 105698. DOI:10.1016/j.cmpb.2020.105698.
18. Almekkaway MK, Shehata IA, Ebbini ES. Anatomical-based model for simulation of HIFU-induced lesions in atherosclerotic plaques. *International Journal of Hyperthermia the Official Journal of European Society for Hyperthermic Oncology North American Hyperthermia Group*. 2015; 31(4):433-42. DOI:10.3109/02656736.2015.1018966.
19. Gupta P, Srivastava A. Numerical analysis of thermal response of tissues subjected to high intensity focused ultrasound. *International Journal of Hyperthermia*. 2018 Dec 31;35(1):419-34. DOI:10.1080/02656736.2018.1506166.
20. Wang M, Zhou Y. High-intensity focused ultrasound (HIFU) ablation by frequency chirp excitation: Reduction of the grating lobe in axial focus shifting. *Journal of Physics D: Applied Physics*. 2018; 51(28):285402. DOI:10.1088/1361-6463/aacaed.
21. Maimbourg G, Houdouin A, Deffieux T, Tanter M, Aubry JF. 3D-printed adaptive acoustic lens as a disruptive technology for transcranial ultrasound therapy using single-element transducers. *Physics in Medicine & Biology*. 2018 Jan 16;63(2):025026. DOI:10.1088/1361-6560/aaa037.
22. Mihcin S, Melzer A. Principles of focused ultrasound. *Minimally Invasive Therapy & Allied Technologies Mitat Official Journal of the Society for Minimally Invasive Therapy*. 2018; 27(1):41-50. DOI:10.1080/13645706.2017.1414063.
23. Dong Z, Zheng H, Zhu Q, Wang Y. Focus prediction of high-intensity focused ultrasound (HIFU) in biological tissue based on magnetic resonance images. *Applied Acoustics*. 2022;197:108927. DOI:10.1016/j.apacoust.2022.108927
24. Qian ZW, Ye S, Fei X, Zhu Z, Jiang W, Yang Y, et al. Shift of Focus Region (SFR) in Heated Tissues by High Intensity Focused Ultrasound (HIFU). *Current Medical Imaging*. 2009 Aug 1;5(3):156-8. DOI:10.2174/157340509789000642.
25. D Li, G Shen, J Bai, Y Chen. Focus shift and phase correction in soft tissues during focused ultrasound surgery[J]. *IEEE transactions on biomedical engineering*. 2011;58(6):1621-8. DOI: 10.1109/TBME.2011.2106210.
26. Suzuki K, Iwasaki R, Takagi R, Yoshizawa S, Umemura SI. Simultaneous observation of cavitation bubbles generated in biological tissue by high-speed optical and acoustic imaging methods. *Japanese journal of applied physics*. 2017 Jun 28;56(7S1):07JF27. DOI:10.7567/JJAP.56.07JF27.
27. Feng G, Hao L, Xu C, Ran H, Zheng Y, Li P, et al. High-intensity focused ultrasound-triggered nanoscale bubble-generating liposomes for efficient and safe tumor ablation under photoacoustic imaging monitoring. *International journal of nanomedicine*. 2017 Jun 28;4647-59. DOI:10.2147/IJN.S135391.
28. Li C, Chen S, Wang Q, et al. Effects of Thermal Relaxation on Temperature Elevation in Ex Vivo tissue During High Intensity Focused Ultrasound[J]. *IEEE Access*, 2020, 8:212013-21.
29. Brotchie A, Grieser F, Ashokkumar M. Effect of Power and Frequency on Bubble-Size Distributions in Acoustic Cavitation. *Physical Review Letters*. 2009; 102(8):084302. DOI:10.1103/PhysRevLett.102.084302.
30. Tsurumi N, Tamura Y, Matsumoto Y. Numerical Simulation of Focused Ultrasound Wave Propagation in Bubbly Fluid Using Equation of Sound Wave. *Transactions of the Japan Society of Mechanical Engineers*. 2012; 78(796):2096-212. DOI:10.1299/kikaib.78.2096.